

1
2
3
4
5
6
7
8
9
10
11
12
13
14
15
16
17
18
19
20
21
22
23
24
25

**Hydrolysis reactions of two benzoyl chlorides as probe to investigate
reverse micelles formed by the ionic liquid-surfactant bmim-AOT**

Nahir Dib^{[a]*}, R. Dario Falcone^[a] and Luis García-Río^{[b]*}

^[a] Instituto para el Desarrollo Agroindustrial y de la Salud (IDAS). CONICET. Departamento de Química. Universidad Nacional de Río Cuarto. Agencia Postal # 3. C.P. X5804BYA Río Cuarto. ARGENTINA.

^[b] Centro Singular de Investigación en Química Biolóxica e Materiais Moleculares (CIQUS) and Departamento de Química Física. Universidade de Santiago de Compostela, 15782 Santiago, SPAIN.

* Corresponding-Authors: Dr. N. Dib. E-mail: ndib@exa.unrc.edu.ar
Prof. L. García-Río. E-mail: luis.garcia@usc.es

26 **ABSTRACT**

27 In this work, two hydrolysis reactions were used as probe to investigate the properties
28 of reverse micelles (RMs) formed by the ionic liquid-surfactant 1-butyl-3-methylimidazolium
29 1,4-bis-2-ethylhexylsulfosuccinate (bmim-AOT). The results were compared with those found
30 for RMs generated with sodium 1,4-bis-2-ethylhexylsulfosuccinate (Na-AOT). As external
31 nonpolar solvents, *n*-heptane (*n*-Hp), isopropyl myristate (IPM) and methyl laurate (ML) were
32 used. Thus, the effect of changing the Na⁺ cation by bmim⁺ was analyzed, as well as the impact
33 of the replacement of a conventional external nonpolar solvent by biocompatible solvents. The
34 kinetics of the hydrolysis reactions of 4-methoxybenzoyl chloride (OMe) and 4-
35 (trifluoromethyl)benzoyl chloride (CF₃) were studied. The results indicate that the replacement
36 of the Na⁺ counterion by bmim⁺ in AOT RMs alters the rates of reactions carried out in them
37 and produces changes in the reaction mechanism. In bmim-AOT RMs, the bmim⁺ cation is
38 located between the surfactant molecules; this has an important influence on the reaction
39 intermediates' stability and, therefore, in the reaction rates and mechanism. Also, the results
40 indicate that when IPM is used as external solvent instead of ML or *n*-Hp, interfacial water
41 molecules have larger nucleophilicity due to the higher interface penetration of IPM.

42

43

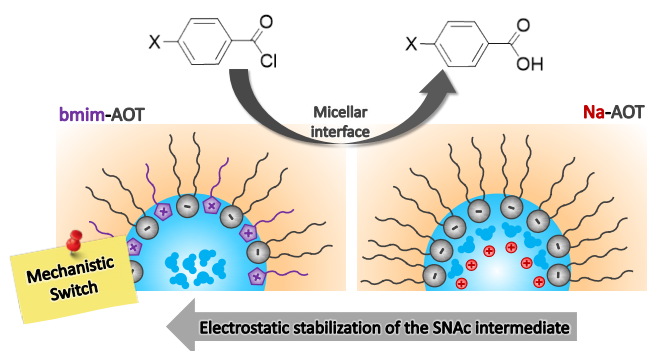
44 **KEYWORDS:** ionic liquid-like surfactant, reverse micelles, nontoxic solvents, hydrolysis,
45 bmim-AOT, benzoyl chloride.

46

47

TABLE OF CONTENTS

48



49

50

51

52

53

54

55

56

57

58

59

60

61

62

63

64

65

66

67

68 1. INTRODUCTION

69 Reverse Micelles (RMs) are aggregates formed by surfactant molecules in a nonpolar
70 organic medium.¹⁻⁴ In these systems, molecules with amphiphilic properties self-assemble so
71 that their polar groups are located towards the interior of the aggregate, while the hydrocarbon
72 chains point outwards, towards the nonpolar solvent. If a third component of polar nature is
73 added, it is encapsulated inside the micellar system. Thus, RMs present three
74 microenvironments: the polar core, the micellar interface, and the external nonpolar phase.⁵

75 The properties of RMs depend on mainly of the type of external nonpolar solvent, the
76 nature of the surfactant, and the confined polar solvent. Based on the nature of the encapsulated
77 solvent, two types of RMs can be defined: aqueous RMs, in which water is encapsulated,⁶⁻¹¹
78 and non-aqueous RMs, in which other polar solvents are confined, such as ethylene glycol,
79 dimethylformamide, ionic liquids (ILs), among other.^{2,12} The external nonpolar solvent can be
80 a traditional solvent, such as *n*-heptane (*n*-Hp), toluene or benzene,^{8,13,14} biocompatible
81 nonpolar solvents, such as isopropyl myristate (IPM) or methyl laurate (ML),¹⁵⁻¹⁷ or
82 hydrophobic ILs.¹⁸ Furthermore, a widely used parameter when studying RMs is *W*, which is
83 defined as the molar ratio between polar solvent and surfactant; when the polar solvent is water,
84 $W=W_0$ and $W_0=[\text{water}]/[\text{surfactant}]$.²

85 ILs are salts formed by large and asymmetric ions; many of them are liquid at room
86 temperature since the attractive forces between the anion and the cation are weak compared to
87 conventional salts.¹⁹⁻²⁵ In general, ILs consist of an organic cation, among the most widely used
88 are 1-alkyl-3-methylimidazolium²⁶⁻²⁸, N-alkyl pyridinium^{29,30}, tetraalkylammonium³¹⁻³³ and an
89 inorganic anion, such as halide anions (Cl⁻, Br⁻, I⁻)³⁴⁻³⁶, tetrafluoroborate [BF₄]⁻,³⁷ bis-
90 (trifluoromethylsulfonyl)imide [NTf₂]⁻³⁷ and hexafluorophosphate [PF₆]⁻.^{37,38}

91 As noted above, ILs can be used in the formation of RMs systems, constituting the
92 external nonpolar phase or the polar core, depending on their properties. Furthermore, there are

93 ILs with amphiphilic properties that can be used as surfactants in the generation of RMs.^{39–44}
94 In these IL-surfactants, at least one of the ions that form it has amphiphilic properties.^{19,45–48}

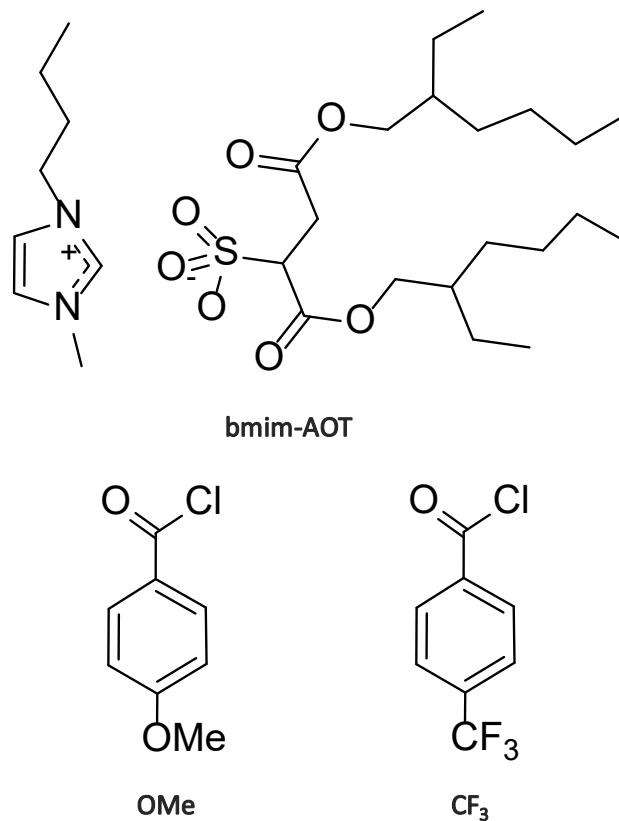
95 In our group, RMs have been generated using different ILs in their composition, either
96 as the polar component or as the surfactant.^{7,8,11,49} One of the IL-surfactants that we have used
97 in the formation of aqueous RMs is 1-butyl-3-methylimidazolium 1,4-bis-2-
98 ethylhexylsulfosuccinate (bmim-AOT, **Scheme 1**).^{7,8,10,11} Traditional nonpolar solvents such as
99 toluene, benzene, chlorobenzene and *n*-Hp were initially used. However, the formation of
100 bmim-AOT RMs using biocompatible nonpolar solvents (IPM and ML) was recently
101 reported,¹¹ with the aim of developing less toxic and more environmentally friendly reverse
102 micellar systems.

103 In the present work, we continue with the study of the properties of bmim-AOT RMs in
104 *n*-Hp, IPM and ML, and its comparison with the micellar systems formed by the traditional
105 surfactant sodium 1,4-bis-2-ethylhexylsulfosuccinate (Na-AOT), using two reactions as probe.
106 The objective is to obtain more information about the interfacial composition and properties of
107 bmim-AOT and Na-AOT RMs, and at the same time, analyze the effect that these systems have
108 when they are used as nanoreactors.

109 Two substrates were used for this study: 4-methoxybenzoyl chloride (OMe) and 4-
110 (trifluoromethyl) benzoyl chloride (CF₃) (**Scheme 1**). This choice is based on the fact that the
111 hydrolysis reaction of these benzoyl chlorides (**Scheme 2**) is very sensitive to the properties of
112 the reaction medium.⁵⁰ Furthermore, the solvolysis of these substrates has been studied in
113 different supramolecular systems, such as direct micelles,^{51,52} vesicles,⁵⁰ and reverse micelles^{53–}
114 ⁵⁵ with very interesting results. In particular, studies in RMs show interesting aspects since both
115 the rate and the mechanism of the reaction are modified.^{53,55–57}

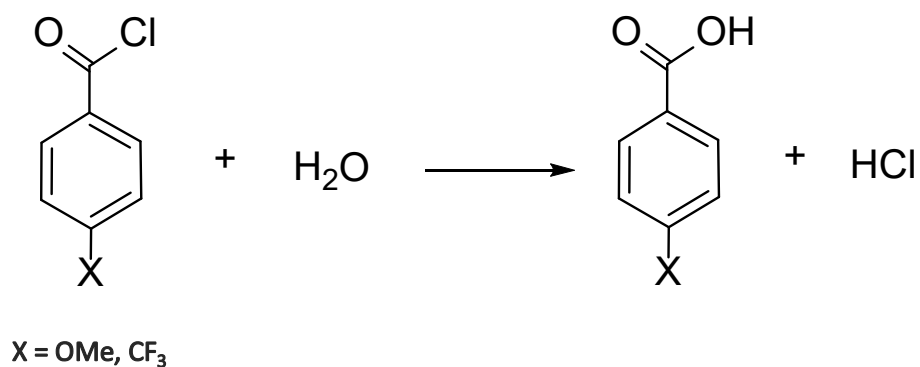
116 Both OMe and CF₃ are very poorly soluble in water, thus it can be assumed that in RMs
117 they are only located in the external nonpolar solvent and/or the micellar interface.⁵⁵ Thus, the

118 hydrolysis reaction only occurs at the interface, where both the substrate and the water are
119 present, allowing to obtain information about the properties of the micellar interface and
120 interfacial water.



121
122 **Scheme 1.** Molecular structure of bmim-AOT and the benzoyl chlorides OMe and CF₃.

123



124

125 **Scheme 2.** Hydrolysis reaction of benzoyl chlorides OMe and CF₃.

126

127

128

129 The obtained results provide kinetic evidence of the different interfacial properties of
130 Na-AOT and bmim-AOT RMs, and the influence of the replacement of the external nonpolar
131 solvent *n*-Hp by the biocompatible IPM and ML. The present work shows that when studying
132 reactions in reverse micellar systems, it is not only important to take into account the effect of
133 the counterion on the properties of interfacial water, but also the location of the counterion in
134 the RM and the impact of this on the stabilization of the reaction intermediate. In some cases,
135 as in the hydrolysis of benzoyl chloride OMe in bmim-AOT RMs, this factor is very important,
136 not only produces changes in the reaction rates but also in the mechanism.

137 Furthermore, the results found evidenced the different penetration of biocompatible
138 external solvents in bmim-AOT RMs, which had not been possible to detect previously by ¹H
139 NMR. Therefore, the present work also shows that the study of the kinetics of the hydrolysis
140 reactions in RMs is an interesting alternative to techniques more commonly used in
141 investigating these micellar systems, such as the ¹H NMR technique.

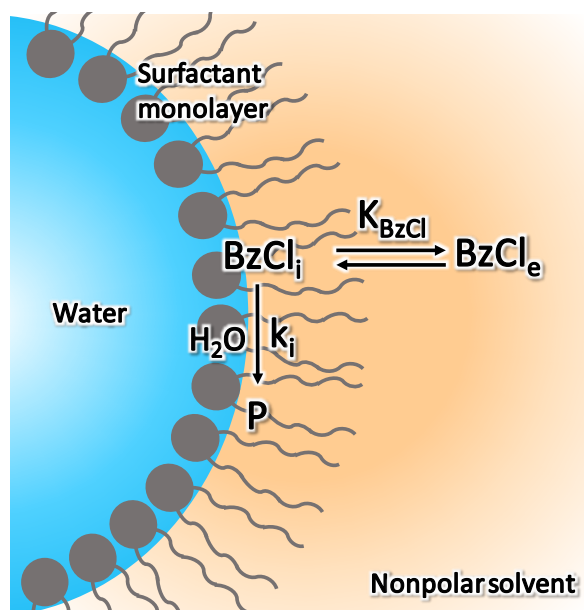
142

143 **2. RESULTS AND DISCUSSION**

144 To determine the kinetic parameters from the experimental data, a model developed in
145 previous works based on the formalism of the micellar pseudophase was used. The pseudophase
146 model was originally developed for direct micelles⁵⁸⁻⁶¹, however, it can be applied to other
147 supramolecular systems such as RMs with satisfactory results. According to this model, the
148 reverse micellar system consists of an aqueous phase, the interface and the continuous nonpolar
149 medium.^{56,62} When a substrate is added to the system, it is located in one or more of the micellar
150 pseudophases according to its solubility. Thus, the overall reaction rate of the substrate is given
151 by the sum of the reaction rates in each pseudophase and will depend on the reagent
152 concentrations in the aqueous phase, the interface and the continuous medium. As noted before,

153 both OMe and CF₃ are poorly soluble in water,⁵⁵ thus it can be assumed that in RMs they are
 154 only present in the external nonpolar solvent and/or the micellar interface. Accordingly, the
 155 hydrolysis reaction only occurs at the interface, where both the substrate and the water are
 156 present (**Scheme 3**).

157



158

159 **Scheme 3.** Benzoyl chloride (BzCl) distribution processes in the reverse micellar system and
 160 location of the reaction. K_{BzCl} is the partition constant of BzCl; k_i is the hydrolysis rate constant
 161 at the micellar interface; BzCl_e and BzCl_i are the substrate located at the external phase and
 162 interface, respectively.

163

164 According to **Scheme 3**, the relationship between the composition of the micellar system
 165 and the pseudo first-order rate constant, k_{obs} , for the hydrolysis of benzoyl chloride is given by
 166 the equation 1^{56,62}:

$$k_{obs} = \frac{k_i K_{BzCl}}{K_{BzCl} + Z} \quad (1)$$

167 where k_i is the rate constant of hydrolysis at the micellar interface and K_{BzCl} is the partition
168 constant of benzoil chloride between the external nonpolar solvent ($BzCl_e$) and the interface
169 ($BzCl_i$):

$$170 \quad K_{BzCl} = \frac{[BzCl]_i}{[BzCl]_e} Z \quad (2)$$

171
172 In equation 2, the concentrations refer to the total volume of the system and Z is defined as $Z =$
173 $[\text{nonpolar solvent}]/[\text{surfactant}]$.

174 Reordering **Equation 1** the following expression is obtained:

$$175 \quad \frac{1}{k_{obs}} = \frac{1}{k_i} + \frac{Z}{k_i K_{BzCl}} \quad (3)$$

176
177 according to which, if $1/k_{obs}$ is plotted as a function of Z parameter, a straight line is obtained
178 whose slope is equal to $1/k_i K_{BzCl}$ and the intercept $1/k_i$; the K_{BzCl} value can be obtained from
179 the relationship between the intercept and the slope. Then, once the K_{BzCl} value is known, the
180 rate constant k_i is obtained through **Equation 1**.

181 Experimentally, the hydrolysis reactions of OMe and CF_3 were followed by monitoring
182 the UV-vis absorbance of the substrate as a function of time and the pseudo first-order rate
183 constant, k_{obs} , was obtained by nonlinear regression of the absorbance-time data, by the
184 integrated first-order rate equation 4:

$$185 \quad A_t = A_0 + (A_\infty - A_0) \exp(-k_{obs} t) \quad (4)$$

186
187
188 where A_0 , A_t , and A_∞ are the absorbances at times 0, t and infinity, respectively.

189 First, the hydrolysis reaction rates of OMe and CF₃ were obtained in bmim-AOT and
190 Na-AOT RMs, varying the surfactant concentration and keeping the water content constant
191 (W₀). Then, K_{BzCl} values for OMe (K_{OMe}) and CF₃ (K_{CF3}) in each micellar system were
192 determined from the experimental data and applying **Equation 3**.

193 Furthermore, a series of experiments were carried out in which the water content (W₀)
194 was varied in order to analyze the influence of the degree of hydration of the micellar interface
195 and the interfacial composition on the reaction rate. The k_{obs} values were obtained under the
196 different experimental conditions and then, with the K_{BzCl} values and **Equation 1**, the k_i values
197 were calculated.

198 The results obtained from the study of the hydrolysis reactions of OMe and CF₃ in
199 bmim-AOT and Na-AOT RMs using *n*-Hp, IPM and ML as nonpolar solvent, following the
200 procedure described, are presented below.

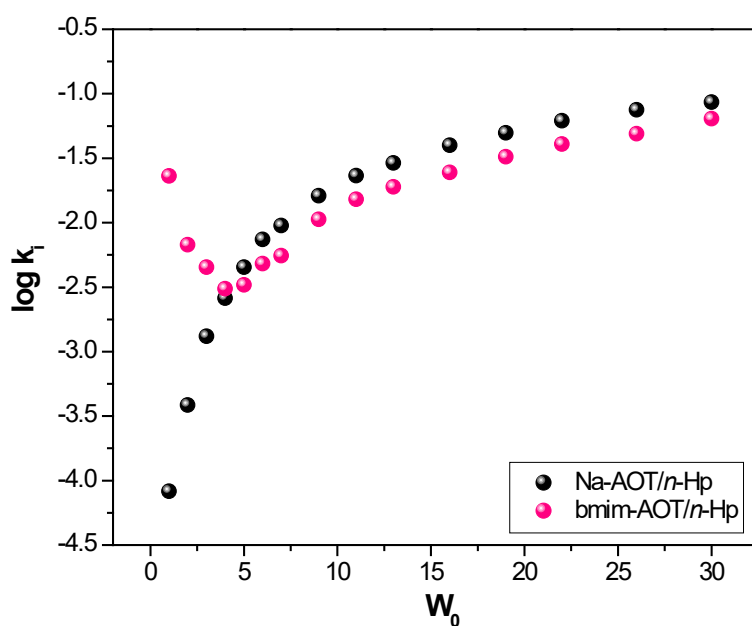
201

202 **2.1. Hydrolysis of OMe**

203 The absorption spectra of a typical run corresponding to the hydrolysis of OMe in Na-
204 AOT/*n*-Hp RMs are shown in **Figure S1**. In Na-AOT/biocompatible solvent, bmim-AOT/*n*-Hp
205 and bmim-AOT/biocompatible solvent RMs the absorption behaviors were similar. Initially, a
206 single band corresponding to the absorption of OMe is observed in the spectrum; then, the
207 absorbance of this band decreases with time and a new band develops at a shorter wavelength
208 that corresponds to the product of the reaction. An isosbestic point between these bands can be
209 observed. The OMe hydrolysis reaction in the RMs was followed by monitoring the
210 disappearance of the reagent at 280-295 nm depending on the micellar system (see pages S11-
211 S201 and S275-S751 of the Supporting Information).

212 As mentioned before, a series of experiments were performed in which the reaction rates
213 of OMe in the RMs were determined at different concentrations of surfactant keeping the water
214 content constant, to calculate the K_{OMe} values (see the Supporting Information).

215 Then, OMe reaction rates in the different micellar systems were determined by varying
216 the water content. From the k_{obs} values obtained in these experiments and the partition constants
217 (Table S1), the values of the rate constant of hydrolysis at the micellar interface, k_i , were
218 calculated using Equation 1. Figure 1 shows the results obtained for the hydrolysis of OMe in
219 Na-AOT/*n*-Hp and bmim-AOT/*n*-Hp RMs. Similar tendencies were found when using IPM and
220 ML as nonpolar external solvents (Figure S4 and S5).



221
222 **Figure 1.** Log k_i as a function of the water content (W_0) for OMe hydrolysis reaction in Na-
223 AOT/*n*-Hp and bmim-AOT/*n*-Hp RMs. $T = 25^\circ\text{C}$.

224
225 As can be seen in Figures 1, S4 and S5, in Na-AOT RMs a gradual increase in the
226 hydrolysis reaction rate occurs with increasing W_0 . Interestingly in bmim-AOT RMs, the
227 observed trend depends on the W_0 range analyzed. At $W_0 > 5$, the reaction rate increases with

228 increasing water content as for Na-AOT systems; however, at $W_0 < 5$ a decrease in the reaction
229 rate is observed when increasing the amount of water confined in the micellar system.

230 Benzoyl chlorides can react with nucleophiles via nucleophilic acyl substitution which
231 involves the formation of a tetrahedral anion intermediate (S_NAc), or through a dissociative
232 mechanism (S_N1), in which an acyl carbocation is formed.^{50,53,55,56} The latter predominates in
233 benzoyl chlorides with electron-donating substituents since they stabilize the carbocation; while
234 the S_NAc mechanism is favored for benzoyl chlorides with electron-withdrawing groups
235 because they stabilize the anionic intermediate.^{50,54}

236 The hydrolysis of OMe generally occurs through a dissociative mechanism (S_N1).^{50,55}
237 In this case, the reaction rate is strongly affected by the polarity of the medium and the ability
238 to stabilize the leaving group.^{50,54-56} Water encapsulated within a reverse micellar system is less
239 polar and less available compared to a continuous aqueous phase,⁶² therefore, the hydrolysis of
240 OMe in the micellar medium is slower than in pure water. Furthermore, the lower the water
241 content in the RMs, greater will be the reduction in the polarity of the encapsulated water.
242 Therefore, in Na-AOT RMs the increase in the hydrolysis rate of OMe with increasing water
243 content (**Figures 1, S4 and S5**) can be attributed to the increasing polarity of the medium.
244 Similar results have been found for water/Na-AOT/isooctane, water/H-AOT/isooctane,⁵⁶ and
245 water/ammonium bis(2-ethylhexyl)phosphate/isooctane⁵⁷.

246 Previous studies of Na-AOT RMs in *n*-Hp, IPM, and ML, using ¹H NMR
247 spectroscopy,^{10,11} reveal that interfacial water molecules interact with the anionic head group
248 of AOT. At low water contents, practically all water molecules are involved in the hydration of
249 the surfactant, through the formation of hydrogen bonds between the hydrogen of the water and
250 the oxygen of the sulfonate group of AOT. Therefore, in addition to the decreasing polarity of
251 the medium, at low W_0 the water molecules are not available for the solvation of the leaving

252 group (Cl^-), which makes the reaction less favorable. Because of this, in Na-AOT RMs, the
253 hydrolysis reaction is slower at low water content.

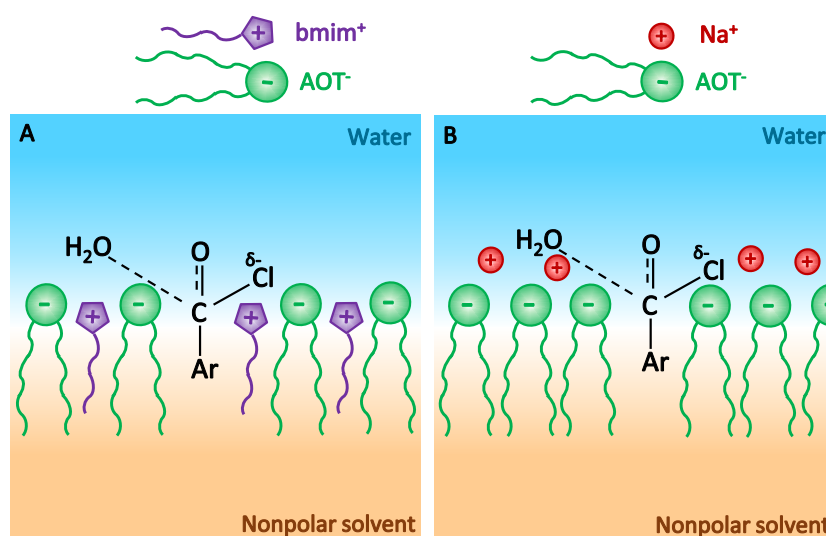
254 In bmim-AOT RMs, the increase in the reaction rate of OMe when the water content is
255 increased for $W_0=5-30$ can also be explained based on the increasing polarity of the
256 encapsulated water and the higher ability to stabilize the Cl^- ion. However, to explain the
257 observed trend at low W_0 values ($W_0<5$), other factors must be considered.

258 Unlike the dissociative mechanism, the rate of the hydrolysis reaction that proceeds
259 through $\text{S}_{\text{N}}\text{Ac}$ mechanism is highly dependent on the nucleophilicity of water.^{50,54-56} In both
260 Na-AOT and bmim-AOT RMs, interfacial water molecules have larger nucleophilicity than
261 bulk water as a result of the interaction with the AOT polar head. As W_0 decreases, the
262 proportion of interfacial AOT-interacting water increases, which could favor water
263 nucleophilicity and thus $\text{S}_{\text{N}}\text{Ac}$ reaction mechanism. In Na-AOT RMs, even at low water
264 contents, the $\text{S}_{\text{N}}1$ mechanism predominates, which is in agreement with the increase in the
265 hydrolysis rate observed when W_0 increases (**Figures 1, S4 and S5**). However, the results
266 suggest that in bmim-AOT RMs, at low W_0 ($W_0<5$) the $\text{S}_{\text{N}}\text{Ac}$ mechanism is more favorable,
267 finding a decrease in the reaction rate when the water content increases. These differences found
268 for Na-AOT and bmim-AOT RMs at low W_0 can be explained taking into account the chemical
269 nature of the surfactant counterion and how this influences the stabilization of the reaction
270 intermediate.

271 The hydrolysis of OMe via nucleophilic acyl substitution involves the formation of an
272 anionic intermediate, therefore, this reaction pathway would be favored in an environment in
273 which the negative charge of the intermediate is stabilized. Considering the more hydrophobic
274 character of bmim^+ compared to Na^+ , in bmim-AOT RMs the bmim^+ cation is part of the
275 surfactant layer. Therefore, the presence of the bmim^+ cation at the micellar interface, which is
276 where the hydrolysis reaction occurs, stabilizes the intermediate with a partial negative charge

277 of the S_NAc mechanism. In contrast, since the Na⁺ counterion is located in the aqueous
278 pseudophase in Na-AOT RMs, the negative charge density at the interface is larger than in the
279 system formed by bmim-AOT (**Scheme 4**); therefore, the increased electrostatic repulsion with
280 the anionic intermediate of the S_NAc mechanism makes the OMe hydrolysis reaction less
281 favorable in Na-AOT RMs.

282



283

284 **Scheme 4.** The bmim⁺ cation at the micellar interface of bmim-AOT RMs stabilizes the
285 intermediate with a partial negative charge of the S_NAc mechanism (A); in Na-AOT RMs, the
286 Na⁺ counterion is located in the aqueous phase therefore the greater negative charge at the
287 interface destabilizes the intermediate (B).

288

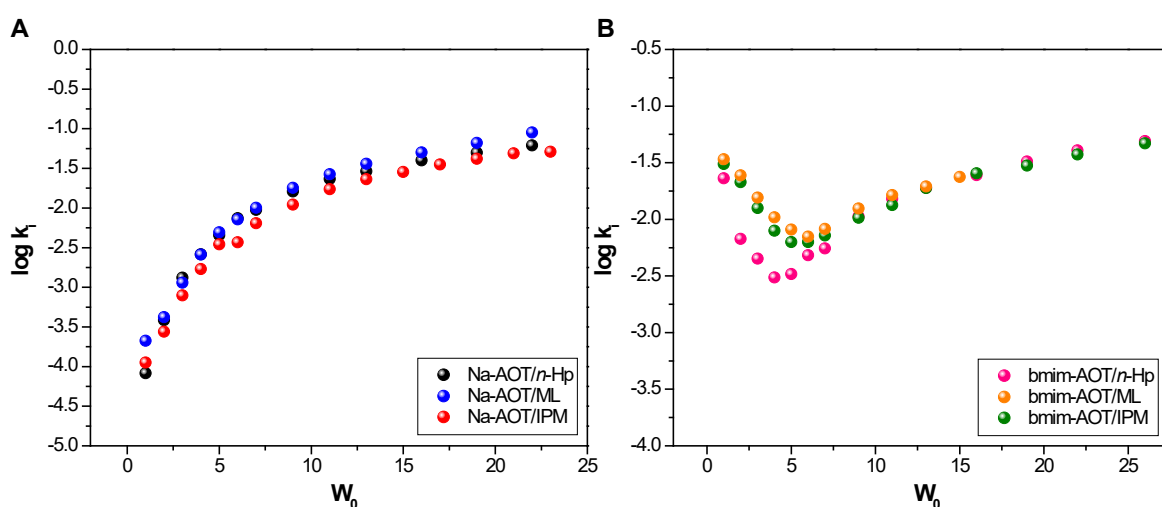
289 In summary, for the hydrolysis of OMe in Na-AOT RMs, the dissociative mechanism
290 predominates in all the range of W_0 analyzed; however, in the micellar systems formed by
291 bmim-AOT, both reaction mechanisms compete, being more favorable the S_NAc mechanism
292 at low water contents and the S_N1 for $W_0 > 5$. Therefore, the replacement of the Na⁺ counterion
293 by bmim⁺ in AOT RMs not only alters the interfacial properties and the reaction rates carried
294 out in them but also produces changes in the reaction mechanism.

295 Previous works have reported a similar mechanistic switch for the hydrolysis of benzoyl
296 chlorides in RMs. In particular, studies of the hydrolysis of benzoyl chloride and 4-
297 methylbenzoyl chloride in water/ammonium bis(2-ethylhexyl) phosphate/isooctane⁵⁷,
298 isooctane/Brij 30/water⁵³ and isooctane/Na-AOT/water⁵⁶ RMs show changes in the reaction
299 mechanism when the water content is varied. Unlike the present work, in these previous reports,
300 the change of mechanism is due to interfacial water properties and the surfactant charge.

301 It is important to note that at $W_0 > 5$, where the S_N1 mechanism predominates in both
302 Na-AOT and bmim-AOT RMs, the reaction rates are slightly larger in the micellar systems
303 formed by the traditional surfactant Na-AOT (**Figure 1, S4 and S5**). This can be attributed to
304 the higher stability of the carbocationic intermediate in Na-AOT RMs, as a result of a larger
305 negative charge density of the micellar interface compared to bmim-AOT RMs, as previously
306 commented.

307 **Figure 2A** shows the $\log k_i$ as a function of water content for the hydrolysis of OMe in
308 Na-AOT RMs in *n*-Hp, IPM and ML, while **Figure 2B** shows the results corresponding to the
309 bmim-AOT systems.

310



311

312 **Figure 2.** Log k_i as a function of the water content (W_0) for OMe hydrolysis reaction in (A)
313 Na-AOT and (B) bmim-AOT RMs, using *n*-Hp, IPM and ML as nonpolar external solvent.

314

315 **Figure 2A** shows that the hydrolysis reaction rate of OMe in Na-AOT RMs practically
316 does not vary when changing the external solvent. In bmim-AOT RMs, there are no differences
317 for $W_0 > 5$ either; however, at low water content ($W_0 < 5$), it is evident that the type of external
318 solvent affects the reaction rate (**Figure 2B**). To explain these results, first, it is necessary to
319 consider the reaction mechanism that predominates in each case.

320 Furthermore, in previous works, it was found that in bmim-AOT RMs, IPM and ML
321 penetrate the micellar interface, unlike *n*-Hp, whereby the ester group of the biocompatible
322 solvent interacts with the bmim⁺ cation which is part of the surfactant monolayer.¹¹ This
323 decreases the bmim⁺-AOT⁻ interaction and increases the negative charge density at the polar
324 head of the surfactant. Consequently, the nucleophilicity of water molecules that interact
325 through hydrogen bonding with AOT also increases. This has a great effect on the reaction rate
326 of the hydrolysis that occurs through S_NAc mechanism. Therefore, this explains why in bmim-
327 AOT RMs, when the predominant mechanism is S_NAc ($W_0 < 5$), higher reaction rates are
328 observed when using IPM and ML instead of *n*-Hp as the external solvent.

329

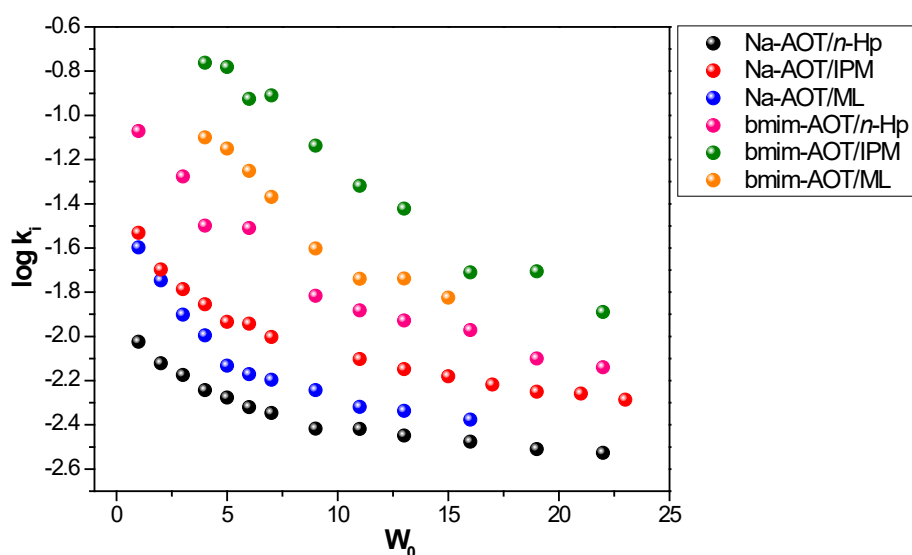
330 **2.2. Hydrolysis of CF₃**

331 In the absorption spectra recorded for the hydrolysis of CF₃ in Na-AOT/*n*-Hp RMs
332 (**Figure S6**), a single band corresponding to the absorption of the substrate is initially observed.
333 The absorbance of this band decreases with time and a new band develops at a shorter
334 wavelength that corresponds to the absorption of the product. The hydrolysis of CF₃ in Na-
335 AOT/biocompatible solvent, bmim-AOT/*n*-Hp and bmim-AOT/biocompatible solvent RMs
336 showed similar tendencies on the spectra. In all cases, the hydrolysis reaction was followed by

337 monitoring the disappearance of the substrate at a wavelength between 293-295 nm depending
338 on the micellar system (see pages S201-S275 and S752-S869 of the Supporting Information).

339 CF_3 hydrolysis rates in the studied micellar systems were determined by varying the
340 surfactant concentration, at constant W_0 , in order to determine K_{CF_3} values (see the Supporting
341 Information). A series of experiments in which the hydrolysis rate was determined at different
342 values of W_0 were also performed. Then the values of k_i were calculated from the experimental
343 data (k_{obs} and K_{CF_3}) and **Equation 1**. The results obtained for the hydrolysis of CF_3 in Na-AOT
344 and bmim-AOT RMs are shown in **Figure 3**.

345



346

347 **Figure 3.** Log k_i as a function of the water content (W_0) for CF_3 hydrolysis reaction in Na-AOT
348 and bmim-AOT RMs, using *n*-Hp, IPM and ML as nonpolar external solvent.

349

350 It can be seen from **Figure 3** that, in all the micellar systems, the reaction rate decreases
351 with increasing water content. This can be understood taking into account that the hydrolysis
352 of benzoyl chlorides with electron-withdrawing substituents, such as CF_3 , generally occurs
353 through an $\text{S}_{\text{N}}\text{Ac}$ mechanism.^{50,55} Therefore, the reaction rate is strongly influenced by the

354 nucleophilic character of the water. In the studied micellar systems, the interfacial water
355 molecules interact with the sulfonate groups of AOT, resulting in an increase in the
356 nucleophilicity of water compared to pure water. At low W_0 , practically all the encapsulated
357 water interacts with the surfactant, therefore, the reaction is faster than at high water contents.
358 As W_0 increases and the hydration of the interface is completed, the amount of free water
359 increases and it begins to recover its hydrogen-bond network structure, thereby decreasing the
360 nucleophilicity of the water molecules. Consequently, increasing the water content decreases
361 the hydrolysis reaction rate of CF_3 .

362 Although a decrease in $\log k_i$ is found in all micellar systems with increasing water
363 content, CF_3 hydrolysis rates vary significantly depending on whether Na-AOT or bmim-AOT
364 RMs are used. For example, at $W_0 = 4$, in bmim-AOT/IPM $k_i = 1.7 \times 10^{-1} \text{ s}^{-1}$, while in Na-
365 AOT/IPM $k_i = 1.4 \times 10^{-2} \text{ s}^{-1}$; in bmim-AOT RMs the reaction rate is more than 10 times larger
366 than in the Na-AOT system. Similar tendencies were found when using *n*-Hp or ML as the
367 external solvent. It is important to note that in bmim-AOT RMs, the nucleophilicity of
368 interfacial water is lower than in Na-AOT.^{8,10,11} Therefore, if only this factor is taken into
369 account, a S_NAc reaction would be expected to be more favorable in Na-AOT than in bmim-
370 AOT RMs. However, this is not what is observed experimentally, as there is another factor that
371 must be taken into account: the counterion $bmim^+$ location compared to Na^+ and the effect of
372 this on stabilizing the reaction intermediate, as previously mentioned.

373 Furthermore, it can be seen that not only the chemical nature of the surfactant affects
374 the reaction rate of CF_3 , but also the identity of the external nonpolar solvent used in the
375 formulation of the RMs. In both bmim-AOT and Na-AOT RMs, hydrolysis reaction rates are
376 larger in biocompatible solvents than in *n*-Hp. This can be explained taking into account the
377 higher biocompatible solvents interface penetration compared to *n*-Hp, and the effect of this on
378 the nucleophilicity of water, as discussed before.

379 Also, from **Figure 3**, it is evident that when using IPM instead of ML, the hydrolysis of
380 CF_3 is faster, both in bmim-AOT and Na-AOT RMs. Previous studies reveal that IPM
381 penetrates more into the interface of reverse micelles than ML, due to its higher viscosity and
382 polarity.^{11,15} This suggests that the interaction of the biocompatible solvent with the counterion
383 of the surfactant is more effective in the case of IPM; thus, the increase in the negative charge
384 density on AOT, and therefore, the increase in nucleophilicity of the water molecules that
385 interact with the surfactant is higher when using IPM instead of ML as the external solvent.
386 Consequently, the reaction rates are higher when using IPM to formulate the RMs.

387 Previously bmim-AOT and Na-AOT RMs were studied through ^1H NMR
388 spectroscopy;¹¹ In these studies, the different penetration of IPM and ML in Na-AOT RMs was
389 evidenced, obtaining different chemical shifts when using each biocompatible solvent.
390 However, in bmim-AOT RMs, chemical shifts were very similar when using IPM and ML;
391 therefore, these ^1H NMR studies did not allow to differentiate the penetration of biocompatible
392 solvents into bmim-AOT systems. Taking into account all the results exposed in the present
393 work, the use of the hydrolysis reaction of CF_3 as a probe allows detecting the different
394 penetration of IPM and ML not only in Na-AOT RMs but also in bmim-AOT RMs.

395

396

397 **3. CONCLUSIONS**

398 The results indicated that the hydrolysis of OMe in Na-AOT RMs occurs through a
399 dissociative mechanism in all the range of W_0 analyzed. However, in the micellar systems
400 formed by bmim-AOT only at $W_0 > 5$ the $\text{S}_{\text{N}}1$ pathway predominates; at low water contents (W_0
401 < 5) the $\text{S}_{\text{N}}\text{Ac}$ mechanism is more favorable, leads to a change of mechanism. These differences
402 between bmim-AOT and Na-AOT are directly related to the chemical nature of the surfactant
403 counter ion and its role in the stabilization of the $\text{S}_{\text{N}}\text{Ac}$ reaction intermediate.

404 In systems formed by Na-AOT, the Na^+ counterion is located in the aqueous
405 pseudophase, while in bmim-AOT, the bmim^+ cation is located at the micellar interface,
406 between the AOT molecules, due to its more hydrophobic character. The presence of bmim^+ at
407 the interface, which is where the hydrolysis reaction occurs, allows stabilizing the anionic
408 intermediate of the $\text{S}_{\text{N}}\text{Ac}$ pathway. Thus, in bmim-AOT RMs at low water contents, where the
409 $\text{S}_{\text{N}}1$ pathway is less favorable, OMe hydrolysis occurs through the $\text{S}_{\text{N}}\text{Ac}$ mechanism.
410 Therefore, the replacement of the Na^+ counterion by bmim^+ in Na-AOT RMs, not only alters
411 the rates of reactions carried out in them but also produces changes in the reaction mechanism.

412 The hydrolysis of CF_3 occurs through an $\text{S}_{\text{N}}\text{Ac}$ mechanism in all the studied micellar
413 systems, showing an increase in reaction rate with decreasing water content. These results were
414 consistent with the fact that, both in Na-AOT and in bmim-AOT RMs, at low W_0 , practically
415 all the water interacts with the polar head of AOT, thus its nucleophilicity is higher compared
416 to pure water. Furthermore, the hydrolysis reactions were faster in bmim-AOT RMs compared
417 to Na-AOT, because the presence of the bmim^+ cation at the interface stabilizes the anionic
418 intermediate.

419 Moreover, when the $\text{S}_{\text{N}}\text{Ac}$ mechanism for the hydrolysis of benzoyl chlorides
420 predominates, the reaction rates are higher when using IPM and ML instead of *n*-Hp as the
421 external solvent. In Na-AOT and bmim-AOT RMs, IPM and ML penetrate the micellar
422 interface, unlike *n*-Hp, whereby the ester group of the biocompatible solvent interacts with the
423 bmim^+ cation that is part of the surfactant monolayer. Consequently, the cation-AOT interaction
424 decreases, and the negative charge density at the polar head of the surfactant increases, thereby
425 increasing the nucleophilicity of the water molecules that interact with AOT. This has a great
426 effect on the rate of hydrolysis reaction that proceeds through an $\text{S}_{\text{N}}\text{Ac}$ mechanism since it
427 strongly depends on the nucleophilicity of the water. Also, the studies indicated that IPM
428 penetrates more the micellar interface than ML, both in Na-AOT and in bmim-AOT RMs.

429 The obtained results provide kinetic evidence of the effect of replacing the Na⁺ cation
430 by bmim⁺ on the composition and interfacial properties of AOT RMs, and the influence of
431 replacing the external solvent *n*-Hp by the biocompatible IPM and ML.

432 The present work shows that when studying reactions in reverse micellar systems it is
433 important to take into account the location of the counterion in the RM and the effect of this on
434 the stabilization of the reaction intermediate. In some cases, as in the hydrolysis of benzoyl
435 chloride OMe in bmim-AOT RMs, this factor is very important, not only produces changes in
436 the reaction rates but also in the mechanism.

437 The obtained results in this work are consistent with those previously found using the
438 ¹H NMR technique and also allowed to detect the different penetration of the biocompatible
439 external solvents in bmim-AOT RMs, which it was not possible by ¹H NMR. Therefore, the
440 use of chemical reactions as a probe is a valuable alternative in investigating the interfacial
441 composition and interfacial properties of RMs, since it is very sensitive to the properties of the
442 medium and is complementary to other techniques, such as NMR.

443

444 **4. EXPERIMENTAL SECTION**

445 **4.1. Materials**

446 The IL bmim-AOT was synthesized in our lab through the procedure previously
447 described⁶³ and Na-AOT was purchased from Sigma (> 99% purity). Both surfactants were
448 dried under vacuum prior to use. ML (≥ 98% purity), IPM (≥ 98% purity) and *n*-Hp (HPLC
449 quality) from Sigma were used without prior purification. Ultrapure water was obtained from
450 Milli-Q (Millipore) equipment. The benzoyl halides OMe and CF₃ from Sigma were of the
451 highest commercially available purity and were used as supplied.

452

453 **4.2. Methods**

454 **Preparation of RMs solutions.** Stock solutions of bmim-AOT and Na-AOT in *n*-Hp, IPM and
455 ML were prepared by mass and volumetric dilution. Individual solutions of RMs were prepared
456 from the stock solutions, incorporating H₂O with calibrated microsyringes. Thus, each reverse
457 micelle solution contains a different amount of water, defined as $W_0 = [\text{water}]/[\text{surfactant}]$.
458 Solutions of different surfactant concentrations were also prepared from the stock solutions,
459 incorporating pure solvent and H₂O. The solutions were shaken in a sonication bath to obtain
460 optically transparent solutions with a single phase.

461 **Kinetic Procedure.** The hydrolysis reaction was followed by monitoring the UV-vis
462 absorbance of the benzoil halide OMe or CF₃, using a Cary 50 UV-Visible Spectrophotometer
463 with thermostated cell holders. The wavelengths used for the kinetic studies fell between 280-
464 295 nm depending on the micellar system. All experiments were carried out at 25 °C. Stock
465 solutions of the benzoil halides in *n*-Hp, IPM and ML were prepared. Appropriate amount of
466 surfactant/nonpolar solvent stock solution and water was transferred into UV-Vis quartz cuvette
467 to obtain the desired micellar system. After thermostating for 10 min, the reaction was initiated
468 by the addition of the benzoil halide from stock solution. The experiments were performed
469 under pseudo first-order conditions where the substrate was always smaller than water
470 concentration ($[\text{OMe}]$ and $[\text{CF}_3] = 1 \times 10^{-4}$ M). The experiments were performed once since
471 previous experiments showed good reproducibility (results could be reproduced with an error
472 margin of 5%).^{56,57} See more details of the kinetic experiments in the supplementary
473 information.

474

475 ASSOCIATED CONTENT

476 **Supporting Information.** Typical UV-vis spectra for the reaction of OMe in the studied RMs
477 (page S3). Determination of K_{OMe} (pages S4-S5). Log k_i as a function of W_0 for OMe hydrolysis
478 in Na-AOT/ML and bmim-AOT/ML RMs (page S6). Log k_i as a function of W_0 for OMe

479 hydrolysis in Na-AOT/IPM and bmim-AOT/IPM RMs (page S7). Typical UV-vis spectra for
480 the reaction of CF₃ in the studied RMs (page S8). Determination of K_{CF₃} (pages S9-S10).
481 Absorbance versus time data for OMe and CF₃ hydrolysis in the studied RMs (pages S11-S869).

482

483 **ACKNOWLEDGMENTS**

484 Financial support from the Consejo Nacional de Investigaciones Científicas y Técnicas
485 (PIP CONICET 112-2015-0100283), Universidad Nacional de Río Cuarto (PPI-UNRC 2016-
486 2019), Agencia Nacional de Promoción Científica y Técnica (PICT 2012-0526, PICT 2015-
487 0585, PICT 2018-0507), and Ministerio de Ciencia y Tecnología, Gobierno de la Provincia de
488 Córdoba (PID 2013, PID 2018) is gratefully acknowledged. R.D.F. holds a research position at
489 CONICET. N.D. thanks CONICET for a research fellowship. LGR thanks the Ministerio de
490 Economía y Competitividad of Spain (project CTQ2017-84354-P), Xunta de Galicia (GR
491 2007/085; IN607C 2016/03 and Centro singular de investigación de Galicia accreditation 2016–
492 2019, ED431G/09) and the European Regional Development Fund (ERDF) is gratefully
493 acknowledged.

494

495 **REFERENCES**

- 496 (1) Langevin, D. Micelles and Microemulsions. *Annu. Rev. Phys. Chem.* **1992**, *43* (1),
497 341–369. <https://doi.org/10.1146/annurev.pc.43.100192.002013>.
- 498 (2) Correa, N. M.; Silber, J. J.; Riter, R. E.; Levinger, N. E. Nonaqueous Polar Solvents in
499 Reverse Micelle Systems. *Chem. Rev.* **2012**, *112* (8), 4569–4602.
500 <https://doi.org/10.1021/cr200254q>.
- 501 (3) Pileni, M. P. Reverse Micelles as Microreactors. *J. Phys. Chem.* **1993**, *97* (27), 6961–
502 6973. <https://doi.org/10.1021/j100129a008>.

- 503 (4) Eastoe, J.; Hollamby, M. J.; Hudson, L. Recent Advances in Nanoparticle Synthesis
504 with Reversed Micelles. *Adv. Colloid Interface Sci.* **2006**, *128–130*, 5–15.
505 <https://doi.org/10.1016/j.cis.2006.11.009>.
- 506 (5) Levinger, N. E.; Swafford, L. A. Ultrafast Dynamics in Reverse Micelles. *Annu. Rev.*
507 *Phys. Chem.* **2009**, *60* (1), 385–406.
508 <https://doi.org/10.1146/annurev.physchem.040808.090438>.
- 509 (6) Baruah, B.; Roden, J. M.; Sedgwick, M.; Correa, N. M.; Crans, D. C.; Levinger, N. E.
510 When Is Water Not Water? Exploring Water Confined in Large Reverse Micelles
511 Using a Highly Charged Inorganic Molecular Probe. *J. Am. Chem. Soc.* **2006**, *128* (39),
512 12758–12765. <https://doi.org/10.1021/ja0624319>.
- 513 (7) Lépori, C. M. O.; Correa, N. M.; Silber, J. J.; Vaca Chávez, F.; Falcone, R. D.
514 Interfacial Properties Modulated by the Water Confinement in Reverse Micelles
515 Created by the Ionic Liquid-like Surfactant Bmim-AOT. *Soft Matter* **2019**, *15* (5), 947–
516 955. <https://doi.org/10.1039/C8SM02217H>.
- 517 (8) Lépori, C. M. O.; Correa, N. M.; Silber, J. J.; Falcone, R. D. How the Cation 1-Butyl-
518 3-Methylimidazolium Impacts the Interaction between the Entrapped Water and the
519 Reverse Micelle Interface Created with an Ionic Liquid-like Surfactant. *Soft Matter*
520 **2016**, *12* (3), 830–844. <https://doi.org/10.1039/C5SM02421H>.
- 521 (9) Zhang, X.; Chen, Y.; Liu, J.; Zhao, C.; Zhang, H. Investigation on the Structure of
522 Water/AOT/IPM/Alcohols Reverse Micelles by Conductivity, Dynamic Light
523 Scattering, and Small Angle X-Ray Scattering. *J. Phys. Chem. B* **2012**, *116* (12), 3723–
524 3734. <https://doi.org/10.1021/jp210902r>.
- 525 (10) Dib, N.; Falcone, R. D.; Acuña, A.; García-Río, L. Characterization of Reverse
526 Micelles Formulated with the Ionic-Liquid-like Surfactant Bmim-AOT and

- 527 Comparison with the Traditional Na-AOT: Dynamic Light Scattering, ¹H NMR
528 Spectroscopy, and Hydrolysis Reaction of Carbonate as a Probe. *Langmuir* **2019**, *35*
529 (39), 12744–12753. <https://doi.org/10.1021/acs.langmuir.9b01083>.
- 530 (11) Dib, N.; Falcone, R. D.; Acuña, A.; García-Río, L. The Ionic Liquid-Surfactant Bmim-
531 AOT and Nontoxic Lipophilic Solvents as Components of Reverse Micelles
532 Alternative to the Traditional Systems. A Study by ¹H NMR Spectroscopy. *J. Mol. Liq.*
533 **2020**, *304*, 112762. <https://doi.org/10.1016/j.molliq.2020.112762>.
- 534 (12) Correa, N. M.; Durantini, E. N.; Silber, J. J. Non-Aqueous Reverse Micelles Media for
535 the SNAr Reaction between 1-Fluoro-2,4-Dinitrobenzene and Piperidine. *J. Phys. Org.*
536 *Chem.* **2006**, *19* (12), 805–812. <https://doi.org/10.1002/poc.1042>.
- 537 (13) Correa, N. M.; Biasutti, M. A.; Silber, J. J. Micropolarity of Reverse Micelles of
538 Aerosol-OT in n-Hexane. *J. Colloid Interface Sci.* **1995**, *172* (1), 71–76.
539 <https://doi.org/10.1006/jcis.1995.1226>.
- 540 (14) Heatley, F. A ¹H Nuclear Magnetic Resonance Chemical-Shift Study of Inverted
541 Microemulsions of Aerosol OT in Benzene and Cyclohexane. Partitioning of Water
542 between Hydrocarbon and Aqueous Phases. *J. Chem. Soc. Faraday Trans. 1 Phys.*
543 *Chem. Condens. Phases* **1988**, *84* (1), 343. <https://doi.org/10.1039/f19888400343>.
- 544 (15) Girardi, V. R.; Silber, J. J.; Mariano Correa, N.; Darío Falcone, R. The Use of Two
545 Non-Toxic Lipophilic Oils to Generate Environmentally Friendly Anionic Reverse
546 Micelles without Cosurfactant. Comparison with the Behavior Found for Traditional
547 Organic Non-Polar Solvents. *Colloids Surfaces A Physicochem. Eng. Asp.* **2014**, *457*,
548 354–362. <https://doi.org/10.1016/j.colsurfa.2014.05.077>.
- 549 (16) Moniruzzaman, M.; Tamura, M.; Tahara, Y.; Kamiya, N.; Goto, M. Ionic Liquid-in-Oil
550 Microemulsion as a Potential Carrier of Sparingly Soluble Drug: Characterization and

- 551 Cytotoxicity Evaluation. *Int. J. Pharm.* **2010**, *400* (1–2), 243–250.
552 <https://doi.org/10.1016/j.ijpharm.2010.08.034>.
- 553 (17) Moniruzzaman, M.; Kamiya, N.; Goto, M. Ionic Liquid Based Microemulsion with
554 Pharmaceutically Accepted Components: Formulation and Potential Applications. *J.*
555 *Colloid Interface Sci.* **2010**, *352* (1), 136–142.
556 <https://doi.org/10.1016/j.jcis.2010.08.035>.
- 557 (18) Moniruzzaman, M.; Kamiya, N.; Nakashima, K.; Goto, M. Formation of Reverse
558 Micelles in a Room-Temperature Ionic Liquid. *ChemPhysChem* **2008**, *9* (5), 689–692.
559 <https://doi.org/10.1002/cphc.200700802>.
- 560 (19) Paul, B. K.; Moulik, S. P. *Ionic Liquid-Based Surfactant Science: Formulation,*
561 *Characterization, and Applications*; John Wiley & Sons, 2015.
- 562 (20) Welton, T. Ionic Liquids: A Brief History. *Biophys. Rev.* **2018**, *10* (3), 691–706.
563 <https://doi.org/10.1007/s12551-018-0419-2>.
- 564 (21) Austen Angell, C.; Ansari, Y.; Zhao, Z. Ionic Liquids: Past, Present and Future.
565 *Faraday Discuss.* **2012**, *154*, 9–27. <https://doi.org/10.1039/C1FD00112D>.
- 566 (22) Egorova, K. S.; Gordeev, E. G.; Ananikov, V. P. Biological Activity of Ionic Liquids
567 and Their Application in Pharmaceutics and Medicine. *Chem. Rev.* **2017**, *117* (10),
568 7132–7189. <https://doi.org/10.1021/acs.chemrev.6b00562>.
- 569 (23) Rogers, R. D.; Voth, G. A. Ionic Liquids. *Acc. Chem. Res.* **2007**, *40* (11), 1077–1078.
570 <https://doi.org/10.1021/ar700221n>.
- 571 (24) Hayes, R.; Warr, G. G.; Atkin, R. Structure and Nanostructure in Ionic Liquids. *Chem.*
572 *Rev.* **2015**, *115* (13), 6357–6426. <https://doi.org/10.1021/cr500411q>.
- 573 (25) Dean, P. M.; Pringle, J. M.; MacFarlane, D. R. Structural Analysis of Low Melting

- 574 Organic Salts: Perspectives on Ionic Liquids. *Phys. Chem. Chem. Phys.* **2010**, *12* (32),
575 9144. <https://doi.org/10.1039/c003519j>.
- 576 (26) Holbrey, J. D.; Seddon, K. R. The Phase Behaviour of 1-Alkyl-3-Methylimidazolium
577 Tetrafluoroborates; Ionic Liquids and Ionic Liquid Crystals. *J. Chem. Soc. Dalt. Trans.*
578 **1999**, No. 13, 2133–2140. <https://doi.org/10.1039/a902818h>.
- 579 (27) Carmichael, A. J.; Seddon, K. R. Polarity Study of Some 1-Alkyl-3-
580 Methylimidazolium Ambient-Temperature Ionic Liquids with the Solvatochromic Dye,
581 Nile Red. *J. Phys. Org. Chem.* **2000**, *13* (10), 591–595. [https://doi.org/10.1002/1099-
582 1395\(200010\)13:10<591::AID-POC305>3.0.CO;2-2](https://doi.org/10.1002/1099-1395(200010)13:10<591::AID-POC305>3.0.CO;2-2).
- 583 (28) Urahata, S. M.; Ribeiro, M. C. C. Structure of Ionic Liquids of 1-Alkyl-3-
584 Methylimidazolium Cations: A Systematic Computer Simulation Study. *J. Chem. Phys.*
585 **2004**, *120* (4), 1855–1863. <https://doi.org/10.1063/1.1635356>.
- 586 (29) Jian-long, W.; ZHAO, D.; ZHOU, E.; DONG, Z. Desulfurization of Gasoline by
587 Extraction with N-Alkyl-Pyridinium-Based Ionic Liquids. *J. Fuel Chem. Technol.*
588 **2007**, *35* (3), 293–296. [https://doi.org/10.1016/S1872-5813\(07\)60022-X](https://doi.org/10.1016/S1872-5813(07)60022-X).
- 589 (30) Cornellas, A.; Perez, L.; Comelles, F.; Ribosa, I.; Manresa, A.; Garcia, M. T. Self-
590 Aggregation and Antimicrobial Activity of Imidazolium and Pyridinium Based Ionic
591 Liquids in Aqueous Solution. *J. Colloid Interface Sci.* **2011**, *355* (1), 164–171.
592 <https://doi.org/10.1016/j.jcis.2010.11.063>.
- 593 (31) Lin, X.-S.; Zou, Y.; Zhao, K.-H.; Yang, T.-X.; Halling, P.; Yang, Z.
594 Tetraalkylammonium Ionic Liquids as Dual Solvents–Catalysts for Direct Synthesis of
595 Sugar Fatty Acid Esters. *J. Surfactants Deterg.* **2016**, *19* (3), 511–517.
596 <https://doi.org/10.1007/s11743-016-1798-7>.

- 597 (32) Anouti, M.; Caillon-Caravanier, M.; Le Floch, C.; Lemordant, D. Alkylammonium-
598 Based Protic Ionic Liquids Part I: Preparation and Physicochemical Characterization. *J.*
599 *Phys. Chem. B* **2008**, *112* (31), 9406–9411. <https://doi.org/10.1021/jp803483f>.
- 600 (33) Jiang, Y.-Y.; Wang, G.-N.; Zhou, Z.; Wu, Y.-T.; Geng, J.; Zhang, Z.-B.
601 Tetraalkylammonium Amino Acids as Functionalized Ionic Liquids of Low Viscosity.
602 *Chem. Commun.* **2008**, No. 4, 505–507. <https://doi.org/10.1039/B713648J>.
- 603 (34) Hunt, P. A.; Kirchner, B.; Welton, T. Characterising the Electronic Structure of Ionic
604 Liquids: An Examination of the 1-Butyl-3-Methylimidazolium Chloride Ion Pair.
605 *Chem. - A Eur. J.* **2006**, *12* (26), 6762–6775. <https://doi.org/10.1002/chem.200600103>.
- 606 (35) Vanyúr, R.; Biczók, L.; Miskolczy, Z. Micelle Formation of 1-Alkyl-3-
607 Methylimidazolium Bromide Ionic Liquids in Aqueous Solution. *Colloids Surfaces A*
608 *Physicochem. Eng. Asp.* **2007**, *299* (1–3), 256–261.
609 <https://doi.org/10.1016/j.colsurfa.2006.11.049>.
- 610 (36) Niedermeyer, H.; Hallett, J. P.; Villar-Garcia, I. J.; Hunt, P. A.; Welton, T. Mixtures of
611 Ionic Liquids. *Chem. Soc. Rev.* **2012**, *41* (23), 7780.
612 <https://doi.org/10.1039/c2cs35177c>.
- 613 (37) Montalbán, M. G.; Bolívar, C. L.; Díaz Baños, F. G.; Villora, G. Effect of
614 Temperature, Anion, and Alkyl Chain Length on the Density and Refractive Index of
615 1-Alkyl-3-Methylimidazolium-Based Ionic Liquids. *J. Chem. Eng. Data* **2015**, *60* (7),
616 1986–1996. <https://doi.org/10.1021/je501091q>.
- 617 (38) Triolo, A.; Russina, O.; Fazio, B.; Triolo, R.; Di Cola, E. Morphology of 1-Alkyl-3-
618 Methylimidazolium Hexafluorophosphate Room Temperature Ionic Liquids. *Chem.*
619 *Phys. Lett.* **2008**, *457* (4–6), 362–365. <https://doi.org/10.1016/j.cplett.2008.04.027>.

- 620 (39) Pal, A.; Maan, R. Micellization Behavior of Anionic Surface Active Ionic Liquid 1-
621 Butyl-3-Methylimidazolium Dodecylbenzenesulfonate in Aqueous Solutions of
622 Nonionic Polymer Polyethylene Glycol: Insights into Competing Mechanisms. *J. Mol.*
623 *Liq.* **2019**, *274*, 183–192. <https://doi.org/10.1016/j.molliq.2018.10.127>.
- 624 (40) Bhat, P. A.; Chat, O. A.; Dar, A. A. Studies on Binary Mixtures of Pluronic P123 and
625 Twin Tailed 1-Butyl-3-Methyl-Imidazolium Aerosol OT - Aggregation Behavior and
626 Impact on Naproxen and Rifampicin Partitioning. *J. Mol. Liq.* **2017**, *241*, 114–122.
627 <https://doi.org/10.1016/j.molliq.2017.05.140>.
- 628 (41) Singh, G.; Singh, G.; Kang, T. S. Micellization Behavior of Surface Active Ionic
629 Liquids Having Aromatic Counterions in Aqueous Media. *J. Phys. Chem. B* **2016**, *120*
630 (6), 1092–1105. <https://doi.org/10.1021/acs.jpcc.5b09688>.
- 631 (42) Pal, A.; Yadav, A. Mixed Micellization of a Trisubstituted Surface Active Ionic Liquid
632 1-Dodecyl-2,3-Dimethylimidazolium Chloride [C12bmim][Cl] with an Amphiphilic
633 Drug Amitriptyline Hydrochloride AMT: A Detailed Insights from Conductance and
634 Surface Tension Measurements. *J. Mol. Liq.* **2019**, *279*, 43–50.
635 <https://doi.org/10.1016/j.molliq.2019.01.107>.
- 636 (43) Sun, S.; Lu, D.; Huang, Q.; Liu, Q.; Yao, Y.; Shi, Y. Reversible Surface Activity and
637 Self-Assembly Behavior and Transformation of Amphiphilic Ionic Liquids in Water
638 Induced by a Pillar[5]Arene-Based Host-Guest Interaction. *J. Colloid Interface Sci.*
639 **2019**, *533*, 42–46. <https://doi.org/10.1016/j.jcis.2018.08.051>.
- 640 (44) Rao, V. G.; Mandal, S.; Ghosh, S.; Banerjee, C.; Sarkar, N. Ionic Liquid-in-Oil
641 Microemulsions Composed of Double Chain Surface Active Ionic Liquid as a
642 Surfactant: Temperature Dependent Solvent and Rotational Relaxation Dynamics of
643 Coumarin-153 in [Py][TF 2 N]/[C 4 Mim][AOT]/Benzene Microemulsions. *J. Phys.*

- 644 *Chem. B* **2012**, *116* (28), 8210–8221. <https://doi.org/10.1021/jp304668f>.
- 645 (45) Ali, M. K.; Moshikur, R. M.; Wakabayashi, R.; Tahara, Y.; Moniruzzaman, M.;
646 Kamiya, N.; Goto, M. Synthesis and Characterization of Choline–Fatty-Acid-Based
647 Ionic Liquids: A New Biocompatible Surfactant. *J. Colloid Interface Sci.* **2019**, *551*,
648 72–80. <https://doi.org/10.1016/j.jcis.2019.04.095>.
- 649 (46) Thoppil, A. A.; Chennuri, B. K.; Gardas, R. L. Insights into the Structural Changes of
650 Bovine Serum Albumin in Ethanolammonium Laurate Based Surface Active Ionic
651 Liquids. *J. Mol. Liq.* **2019**, *290*, 111229. <https://doi.org/10.1016/j.molliq.2019.111229>.
- 652 (47) Mustahil, N. A.; Baharuddin, S. H.; Abdullah, A. A.; Reddy, A. V. B.; Abdul Mutalib,
653 M. I.; Moniruzzaman, M. Synthesis, Characterization, Ecotoxicity and
654 Biodegradability Evaluations of Novel Biocompatible Surface Active Lauroyl
655 Sarcosinate Ionic Liquids. *Chemosphere* **2019**, *229*, 349–357.
656 <https://doi.org/10.1016/j.chemosphere.2019.05.026>.
- 657 (48) Dai, X.; Qiang, X.; Li, J.; Yao, T.; Wang, Z.; Song, H. Design and Functionalization of
658 Magnetic Ionic Liquids Surfactants (MILSs) Containing Alkyltrimethylammonium
659 Fragment. *J. Mol. Liq.* **2019**, *277*, 170–174.
660 <https://doi.org/10.1016/j.molliq.2018.12.096>.
- 661 (49) Blach, D.; Pessêgo, M.; Silber, J. J.; Correa, N. M.; García-Río, L.; Falcone, R. D.
662 Ionic Liquids Entrapped in Reverse Micelles as Nanoreactors for Bimolecular
663 Nucleophilic Substitution Reaction. Effect of the Confinement on the Chloride Ion
664 Availability. *Langmuir* **2014**, *30* (41), 12130–12137.
665 <https://doi.org/10.1021/la501496a>.
- 666 (50) Cabaleiro-Lago, C.; Garcia-Río, L.; Hervés, P.; Pérez-Juste, J. Effects of Zwitterionic
667 Vesicles on the Reactivity of Benzoyl Chlorides. *J. Phys. Chem. B* **2006**, *110* (16),

- 668 8524–8530. <https://doi.org/10.1021/jp060683q>.
- 669 (51) Bunton, C. A.; Gillitt, N. D.; Mhala, M. M.; Moffatt, J. R.; Yatsimirsky, A. K. Micellar
670 Charge Effects upon Hydrolyses of Substituted Benzoyl Chlorides. Their Relation to
671 Mechanism †. *Langmuir* **2000**, *16* (23), 8595–8603. <https://doi.org/10.1021/la000109k>.
- 672 (52) Bunton, C. A. Micellar Charge Effects as Mechanistic Criteria in Spontaneous
673 Hydrolyses of Acid Chlorides. *J. Phys. Org. Chem.* **2005**, *18* (2), 115–120.
674 <https://doi.org/10.1002/poc.747>.
- 675 (53) Campos-Rey, P.; Cabaleiro-Lago, C.; Hervés, P. Promoting Mechanistic Changes:
676 Solvolysis of Benzoyl Halides in Nonionic Microemulsions. *J. Phys. Chem. B* **2009**,
677 *113* (35), 11921–11927. <https://doi.org/10.1021/jp9039463>.
- 678 (54) Campos-Rey, P.; Cabaleiro-Lago, C.; Hervés, P. Solvolysis of Substituted Benzoyl
679 Chlorides in Nonionic and Mixed Micellar Solutions. *J. Phys. Chem. B* **2010**, *114* (44),
680 14004–14011. <https://doi.org/10.1021/jp107538v>.
- 681 (55) García-Río, L.; Leis, J. R. Microemulsion-Promoted Changes of Reaction Mechanisms:
682 Solvolysis of Substituted Benzoyl Chlorides. *Chem. Commun.* **2000**, No. 6, 455–456.
683 <https://doi.org/10.1039/a909531d>.
- 684 (56) Fernández, E.; García-Río, L.; Parajó, M.; Rodríguez-Dafonte, P. Influence of Changes
685 in Water Properties on Reactivity in Strongly Acidic Microemulsions. *J. Phys. Chem. B*
686 **2007**, *111* (19), 5193–5203. <https://doi.org/10.1021/jp0706073>.
- 687 (57) García-Río, L.; Hervella, P.; Rodríguez-Dafonte, P. Solvolysis of Benzoyl Halides in
688 Water/NH₄ DEHP/Isooctane Microemulsions. *Langmuir* **2006**, *22* (18), 7499–7506.
689 <https://doi.org/10.1021/la0606953>.
- 690 (58) Romsted, L. S. Surfactants in Solution; Mitta, K. L., Lindman, B., Eds.; Plenum Press:

- 691 New York, 1984; Vol. 2, p 1015.
- 692 (59) Bunton, C. A.; Savelli, G. Organic Reactivity in Aqueous Micelles and Similar
693 Assemblies; 1986; pp 213–309. [https://doi.org/10.1016/S0065-3160\(08\)60169-0](https://doi.org/10.1016/S0065-3160(08)60169-0).
- 694 (60) Bunton, C. A. Reaction Kinetics in Aqueous Surfactant Solutions. *Catal. Rev.* **1979**, *20*
695 (1), 1–56. <https://doi.org/10.1080/03602457908065104>.
- 696 (61) Quina, F. H.; Chaimovich, H. Ion Exchange in Micellar Solutions. 1. Conceptual
697 Framework for Ion Exchange in Micellar Solutions. *J. Phys. Chem.* **1979**, *83* (14),
698 1844–1850. <https://doi.org/10.1021/j100477a010>.
- 699 (62) Garcia-Rio, L.; Leis, J. R.; Iglesias, E. Influence of Water Structure on Solvolysis in
700 Water-in-Oil Microemulsions. *J. Phys. Chem.* **1995**, *99* (32), 12318–12326.
701 <https://doi.org/10.1021/j100032a041>.
- 702 (63) Brown, P.; Butts, C. P.; Eastoe, J.; Fermin, D.; Grillo, I.; Lee, H.-C.; Parker, D.; Plana,
703 D.; Richardson, R. M. Anionic Surfactant Ionic Liquids with 1-Butyl-3-Methyl-
704 Imidazolium Cations: Characterization and Application. *Langmuir* **2012**, *28* (5), 2502–
705 2509. <https://doi.org/10.1021/la204557t>.
- 706